© 2021. This manuscript version is made available under the CC-BY-NC-ND 4.0 license http://creativecommons.org/licenses/by-nc-nd/4.0/

Electrical and thermal performance comparison between PVT-ST and PV-ST systems

Zhonghe Han[a]

Kaixin Liu[a]

Guiqiang Li[b, *]

Guiqiang.Li@hull.ac.uk

Xudong Zhao[b]

Samson Shittu[b]

[a]Department of Power Engineering, School of Energy, Power and Mechanical Engineering, North China Electric Power University, Baoding, 071003, China

[b]Research Centre for Sustainable Energy Technologies, University of Hull, Hull, HU6 7RX, UK

*Corresponding author.

Abstract

Both photovoltaic (PV), and photovoltaic thermal (PVT) are technologies that use solar energy for power output. Combining them with solar thermal (ST) can enable the generation of electricity as well as high-temperature hot water. In this study, The heat transfer model was established to investigate the thermal, electrical and overall performance of the two systems, which one is a separately operating PV and ST system (i.e. PV-ST system) and the other is a PVT and ST system in series (i.e. PVT-ST). By comparing the electrical, thermal and overall performance of the two combinations under different solar radiation, ambient temperature and inlet temperature, the application range, advantages and disadvantages of the two combinations are given, which can provide guidance for the design of higher electrical and thermal output system. The comparative study of the two systems shows that the electrical efficiency, thermal efficiency and primary energy saving efficiency of the PV-ST system are higher than that of the PVT-ST system under the conditions of low ambient temperature and solar radiation. This makes the PV-ST system have a wider application prospect in such low temperature and weak radiation environment conditions. However, under the environmental conditions of higher ambient temperature and stronger solar radiation intensity, the electro-thermal efficiency and primary energy saving efficiency of PVT-ST system will be higher than that of PV-ST system. The PVT-ST system will be widely used in high temperature and strong radiation conditions.

Keywords: Photovoltaic; PVT; Electrical and thermal; Performance comparison; Heat transfer

1 Introduction

The demand for energy in human society is increasing with the improvement of human living standards and rapid industrialization. The engineering industry is more eager to find sustainable and cheap energy as people pay more attention to the environmental impacts related to energy production and the trend of rising energy prices [1].

It is important to explore renewable energy that can be used as alternatives to meet the growing energy demand [2,3]. Notably, solar energy has obvious advantages over other types of renewable energy as it is easy to be obtained, massive, and inexhaustible [4]. Its availability greatly exceeds any possible future energy demand [5]. Therefore, this kind of clean energy is favored by governments and scientists of various countries.

Photovoltaic is a method of converting solar energy into electrical energy. However, the electrical efficiency of current PV cells is still relatively low. Under the reference test conditions, the electrical efficiency of typical commercial PV cells is only 6.0 %–25.0 % [6]. Most of the remaining solar energy is converted into heat energy, which makes the temperature of photovoltaic panels rise and the electrical efficiency decreases. Therefore, researchers have proposed a photovoltaic thermal (PVT) module, which integrates PV and ST. In the PVT module, the PV panel is cooled through the flow of water, which can reduce the PV temperature and improve electrical efficiency, and can also produce hot water. The PVT module can provide more energy output compared with a single PV module or a single solar collector in the same area [7].

In recent decades, researchers from all over the world have conducted a large number of experiments and simulations to study the performance of different PVT modules [8–18]. Pang et al. [8] used CFD numerical simulation to establish a simplified thermal transfer model and verified its practicability through experiments, thus presenting a new method for finding efficient PVT modules. Dhimish [9] analyzed 8000 photovoltaic systems distributed throughout the UK. The effect of seasonal heat on the performance of photovoltaic systems was investigated, and the conclusion was that the monthly PR rate in spring and summer will be higher than in autumn and winter. Finally, detailed experiments were carried out on three different photovoltaic modules affected by different hot spots. El Fouas et al. [10] proposed a new type of photovoltaic thermal solar power plant numerical model which was verified by experimental data. The simulation was carried out by MATLAB, accounting for the influence of solar radiation, outdoor temperature, wind speed, heat storage temperature, flow rate and characteristics of photovoltaic solar panels on electricity and thermal energy. Barone et al. [11] developed a special dynamic simulation tool to conduct a comprehensive analysis of two architectural PVT prototypes. The results show that the tool can perform a complete system performance analysis, showing the capabilities of the proposed innovative device and the capabilities of the proposed internal code. Sun et al. [12] proposed a new method for calculating the nominal operating cell temperature (NOCT) of PVT modules using water as the working fluid. Under the condition of a clear sky in Chiang Mai, Thailand, this method is in good agreement with the experimental data. Das et al. [13] developed a new type of PVT system model which includes the thermal resistance of each layer and the contact thermal resistance between them in detail, and the agreement is well verified by experiments. Based on this model, the experimental electrical efficiency, thermal efficiency, and exergy efficiency was accurately predicted. Kant et al. [14] proposed a new method for predicting the thermal performance of photovoltaic panels which were verified by experiments. In addition, two cities in India were simulated by the same model and found that they have great potential for installing solar photovoltaic thermal technology. Sardouei et al. [15] used a three-dimensional computational fluid dynamics (CFD) model to analyze three different types of PVT absorbers: round tubes and absorber plates, square tubes and absorber plates, and box-type PVT absorbers. Numerical simulations were performed to close the loopholes about these types of insufficient research. Photovoltaic thermal (PVT) modules can generate electricity and thermal energy at the same time, but the outlet temperature should not be too high. The efficiency of the photovoltaic cell will decrease as the temperature rises, resulting in a decline in photoelectric performance [16,17]. To further increase the temperature, Ma et al. [18] proposed an innovative integrated system called PVT-ST that connects PVT modules in series with subsequent solar thermal (ST) absorbers. This model can overcome the drawback of low output temperature of PVT and not generating electricity for ST.

However, solar absorbers are often connected to a water tank to form a circulating hot water heating system in practical applications, so the inlet temperature will continue to increase instead of remaining at a lower temperature. Therefore, the system has certain shortcomings when the inlet water temperature is high. The electrical efficiency of the independent PV system which can be cooled by the ambient will not be influenced by the inlet water temperature. The cooling effect will be better than that of the PVT system with a glass cover in winter or cold regions. Therefore, the independent PV system will have a higher electrical efficiency than PVT systems.

The pros and cons of the PV and ST operating separately system (PV-ST) and the PVT and ST connection system (PVT-ST) cannot be directly determined in the case of obtaining the same electricity or the same thermal energy output. This is particularly important in the design and high-performance output of solar energy systems. However, there are few related comparison studies presently.

This paper compares the electricity and thermal energy output performance of PV-ST and PVT-ST systems with the same total receiving area under different environmental conditions. The application scope, pros and cons of the two combinations are presented through the comparison of electrical and thermal performance under the different solar irradiations, ambient temperature and inlet temperature, which will provide guidance for the design of the higher electrical power and thermal output system.

2 Concept and configuration

The PVT-ST system consists of a PVT module, ST absorber, and water tank, which are connected in series as a whole system. The schematic diagram of the PVT-ST system is shown in Fig. 1. Part of the solar radiation reaches the solar cell and is converted into electricity in the PVT module, and the rest is converted into thermal energy. Part of this thermal energy is lost to the ambient, and the rest is absorbed by circulating water. The preheated water from the PVT module flows into the subsequent ST module for reheating, and finally outputs high temperature water.

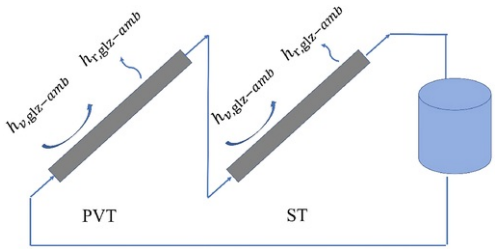

Fig. 1 Schematic diagram of PVT-ST system.

alt-text: Fig. 1

The PV-ST system consists of a PV module, ST absorber, and water tank. The schematic diagram of the PV-ST system is shown in Fig. 2. The ST module is connected in series with the water tank, and the PV module operates independently. Solar radiation is directly impinged on the PV module without cover and converted into electricity. The circulating water only passes through the ST system to produce hot water. The PVT-ST and PV-ST systems maintain the same total receiving area.

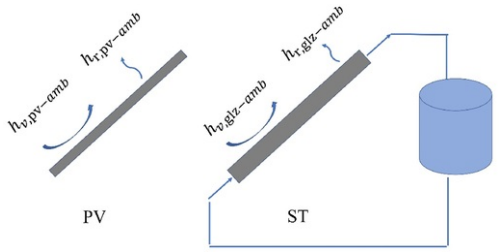

Fig. 2 Schematic diagram of PV-ST system.

alt-text: Fig. 2

The main parameters of the PVT-ST and PV-ST system are listed in Table 1.

Table 1 Main parameters of the PVT-ST and PV-ST system [18].

alt-text: Table 1

Parameters		Value
Thickness (m)	Glass	0.004
	PV module	0.0058
	Absorber	0.0003
	Insulation	0.035
Glazing spacing (m)		0.025
Type of PV modules		JKM285PP-60-DV, Jinko Solar
Number of cells		60
Maximum power rating (W)		285
Nominal efficiency of PV module (%)		17.8
Temperature coefficient of PV modules (%/°C)		−0.38
Diameter of tube (m)		0.01
Tube number		10
Tube spacing		0.1
Collector area of PVT module (m^2)		1.65 (1.658 m × 0.992 m)
Collector area of ST collector (m^2)		1.65 (1.658 m × 0.992 m)
Slope		30°

3 Methodology

In this section, the mathematical model of the three main modules is established to conduct numerical simulation and performance evaluation in the following sections.

The schematic diagram of the energy transfer process of the PVT module is shown in Fig. 3. Part of the solar energy absorbed by the PV panel is converted into electricity, and most of it is converted into thermal energy. Part of this thermal energy is lost to the ambient through radiation and convection, and the rest is taken away by the circulating water.

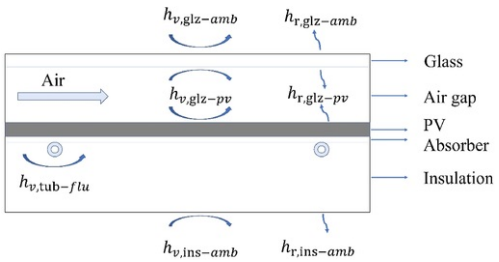

Fig. 3 Schematic diagram of PVT energy transfer process.

alt-text: Fig. 3

The heat exchange process of the ST module is similar to that of the PVT module, but there is no photovoltaic structure. Most of the thermal energy converted from the solar energy which is absorbed by ST is taken away by the circulating water and the other part is lost to the ambient through convection and radiation. The schematic diagram of the energy transfer process is shown in Fig. 4.

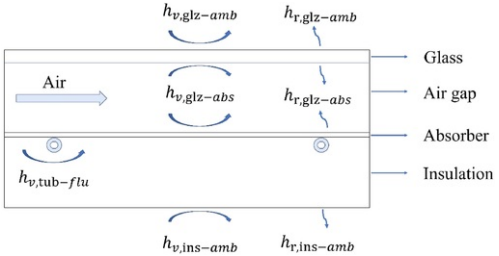

Fig. 4 Simplified diagram of ST energy transfer process.

alt-text: Fig. 4

The energy transfer process of the PV module is shown in Fig. 5. The PV module is completely exposed to the air, part of the solar energy absorbed by the PV is converted into electricity, and of the remaining solar energy most of it is lost to the ambient through radiation and convection.

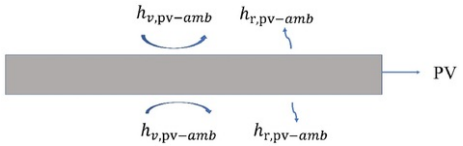

Fig. 5 Schematic diagram of PV energy transfer process.

alt-text: Fig. 5

In order to simplify the numerical simulation process, the following assumptions are made:

(1) The thermal resistance loss inside the photovoltaic module is negligible;

(2) The thermophysical properties of different layers remain unchanged;

(3) Only one of the ten parallel tubes is considered;

(4) Between the circulating water and the water pipe, there is no frictional resistance;

(5) The influence of dust and dirt is ignored.

3.1 Mathematical model

3.1.1 PV

Both the upper and lower surfaces of the PV panel are exposed to the air and heat loss through convection and radiation. Therefore, the energy conservation equation is:

$$\alpha_{pv}G-\left(h_{v,pv-amb}+h_{r,pv-amb}\right)\left(T_{pv}-T_{amb}\right)\times 2-E_{ele,pv}+K_{pv}\delta_{pv}\left(\frac{\partial^2 T_{pv}}{\partial x^2}+\frac{\partial^2 T_{pv}}{\partial y^2}\right)=0 \quad (1)$$

where

$$E_{ele,pv}=G\eta_{ref}\left[1-\beta\left(T_{pv}-T_{ref}\right)\right] \quad (2)$$

α_{pv} is the absorptivity of the PV panel; $E_{ele,pv}$ is the electricity output per unit area of the PV module; where η_{ref} is the electrical efficiency of the PV panel at the reference temperature; β is the temperature coefficient; T_{ref} is the reference temperature. G is the solar radiation; $h_{v,pv-amb}$ and $h_{r,pv-amb}$ respectively represent the convective and radiative coefficient between the PV panel and the ambient; T_{pv} and T_{amb} respectively represent the PV panel temperature and the ambient temperature; K_{pv} is the thermal conductivity of the PV panel; δ_{pv} is the thickness of the PV panel; $\left(\frac{\partial^2 T_{pv}}{\partial x^2}+\frac{\partial^2 T_{pv}}{\partial y^2}\right)$ is the temperature distribution of the PV panel.

3.1.2 PVT

PVT module heat exchange components are mainly divided into: (1) Glass cover; (2) PV module; (3) Absorber; (4) Tube; (5) Circulating water; and (6) Insulation. The energy balance equation of each layer is expressed as follows:

- Glass cover: The glass cover in the PVT module absorbs a small part of solar energy and converts it into heat. The glass cover also has radiative and convective heat exchange with the PV module and the ambient. The energy conservation equation is:

$$\alpha_{gla1}G-h_{v,gla1-amb}\left(T_{gla1}-T_{amb}\right)-\left(h_{v,gla1-pv}+h_{r,gla1-pv}\right)\left(T_{gla1}-T_{pv}\right)-h_{r,gla1-sky}\left(T_{gla1}-T_{sky}\right)+K_{gla1}\delta_{gla1}\left(\frac{\partial^2 T_{gla1}}{\partial x^2}+\frac{\partial^2 T_{gla1}}{\partial y^2}\right)=0 \quad (3)$$

where α_{gla1} is the absorptivity of the glass cover; $h_{v,gla1-amb}$ is the convective coefficient between the glass cover and the ambient; $h_{v,gla1-pv}$ and $h_{r,gla1-pv}$ are the convective and radiative coefficients between the glass cover and the PV module; $h_{r,gla1-sky}$ is the radiative coefficient between the glass cover and the sky; T_{gla1}, T_{amb}, T_{pv} and T_{sky} are the glass cover temperature, ambient temperature, PV temperature, sky equivalent temperature; K_{gla1} is the thermal conductivity of the glass cover; δ_{gla1} is the thickness of the glass cover; $\left(\frac{\partial^2 T_{gla1}}{\partial x^2}+\frac{\partial^2 T_{gla1}}{\partial y^2}\right)$ is the temperature distribution of the glass cover.

In addition, the temperature of sky can be obtained as [19].

$$T_{sky}=0.05527T_{amb}^{1.5} \quad (4)$$

- PV module: In order to simplify the heat exchange process, the PV module is regarded as an integral module. The simplified PV module and the glass cover exchange heat through convection and radiation, and the collector exchanges heat through heat conduction. The energy conservation equation is:

$$\alpha_{pv,e}G-h_{c,pv-abs1}\left(T_{pv}-T_{abs1}\right)+\left(h_{v,gla1-pv}+h_{r,gla1-pv}\right)\left(T_{gla1}-T_{pv}\right)-E_{ele}+K_{pv}\delta_{pv}\left(\frac{\partial^2 T_{pv}}{\partial x^2}+\frac{\partial^2 T_{pv}}{\partial y^2}\right)=0 \quad (5)$$

where $\alpha_{pv,e}$ represents the effective absorptivity of the PV module. Considering the transmittance of the glass cover, the calculation formula is:

$$\alpha_{pv,e}=\tau_{gla1}\alpha_{pv} \quad (6)$$

In addition, $h_{c,pv-abs1}$ is the conductive coefficient between PV and absorber; $h_{v,gla1-pv}$ and $h_{r,gla1-pv}$ are the convective and radiative coefficients between the glass cover and PV, respectively; T_{abs1} is the absorber temperature;

$\left(\frac{\partial^2 T_{pv}}{\partial x^2}+\frac{\partial^2 T_{pv}}{\partial y^2}\right)$ is the temperature distribution of the PV panel.

E_{ele} is the electricity output per unit area of the PV module, which is related to the temperature coefficient and can be derived from the specifications of the PV module [20]. The expression is:

$$E_{ele}=\tau_{gla}G\eta_{ref}\left[1-\beta\left(T_{pv}-T_{ref}\right)\right] \quad (7)$$

where η_{ref} is the electrical efficiency of the PV panel at the reference temperature; β is the temperature coefficient; T_{ref} is the reference temperature.

■ Absorber: For the absorber of the PVT module, there is only conduction between the PV panel, the tube, and the insulation in contact with it. The energy conservation equation is:

$$\begin{aligned}&\alpha_{abs1,e}G-h_{c,pv-abs1}\left(T_{pv}-T_{abs1}\right)-\frac{A_{abs1-tub1}}{A_{abs1}}h_{c,abs1-tub1}\left(T_{abs1}-T_{tub1}\right)\\&-h_{c,abs1-ins1}\left(T_{abs1}-T_{ins1}\right)+K_{abs1}\delta_{abs1}\left(\frac{\partial^2 T_{abs1}}{\partial x^2}+\frac{\partial^2 T_{abs1}}{\partial y^2}\right)=0\end{aligned} \quad (8)$$

where $\alpha_{abs1,e}$ is the effective absorptivity of the absorber, which is related to the transmittance of the glazing cover and PV module glass, and the expression is:

$$\alpha_{abs1,e}=\tau_{gla1}\tau_{pvcell}\alpha_{abs1} \quad (9)$$

In addition, $h_{c,pv-abs1}$ is the conductive coefficient between PV and absorber; $h_{c,abs1-tub1}$ is the conductive coefficient between absorber and tube; $h_{c,abs1-ins1}$ is the conductivity coefficient between absorber and insulation; $A_{abs1-tub1}$ is the contact area between absorber and tube and A_{abs1} is the area of absorber; K_{abs1}, δ_{abs1} and $\left(\frac{\partial^2 T_{abs1}}{\partial x^2}+\frac{\partial^2 T_{abs1}}{\partial y^2}\right)$ are the thermal conductivity, thickness, and temperature distribution of the absorber, respectively; T_{abs1}, T_{tub1} and T_{ins1} are the temperature of the absorber, tube, and insulation, respectively.

■ Tube: There is conduction heat exchange between the tube and the absorber and insulation, and there is convection with the circulating water in the tube. The energy conservation equation of one of the tubes is:

$$\begin{aligned}&A_{abs1-tub1}h_{c,abs1-tub1}\left(T_{abs1}-T_{tub1}\right)-A_{tub1-ins1}h_{c,tub1-ins1}\left(T_{tub1}-T_{ins1}\right)\\&-A_{tub1-flu1}h_{v,tub1-flu1}\left(T_{tub1}-T_{flu1}\right)+K_{tub1}\frac{p\left(D_0^2-D_i^2\right)}{4}\frac{d^2T_{tub1}}{dy^2}=0\end{aligned} \quad (10)$$

where $A_{tub1-ins1}$ is the contact area between tube and insulation; $A_{tub1-flu1}$ is the contact area between tube and fluid; $h_{c,tub1-ins1}$ is the conductive coefficient between tube and insulation; $h_{v,tub1-flu1}$ is the convective coefficient between tube and fluid; T_{flu1} is the temperature of fluid; K_{tub1} is the thermal conductivity of tube; $\frac{d^2T_{tub1}}{dy^2}$ is the temperature distribution of tube.

■ Circulating water: The circulating water in the tube only has convection heat exchange with the tube, so the energy conservation equation is:

$$A_{tub1-flu1}h_{v,tub1-flu1}\left(T_{tub1}-T_{flu1}\right)-C_{flu1}\dot{m}_{flu1}\frac{dT_{flu1}}{dy}=0 \quad (11)$$

where C_{flu1} is the specific heat capacity of fluid; $\dot{m}_{flu1}$ is the mass flow of fluid; $\frac{dT_{flu1}}{dy}$ is the temperature distribution of fluid.

■ Insulation: There is conductive heat exchange between the insulation and the absorber and tube, and there is convection and radiation heat exchange with the ambient. The energy conservation equation is:

$$\begin{aligned}&\frac{A_{tub1-ins1}}{A_{ins1}}h_{c,tub1-ins1}\left(T_{tub1}-T_{ins1}\right)+h_{c,abs1-ins1}\left(T_{abs1}-T_{ins1}\right)\\&-h_{v,ins1-amb}\left(T_{ins1}-T_{amb}\right)+K_{ins1}\delta_{ins1}\left(\frac{\partial^2 T_{ins1}}{\partial x^2}+\frac{\partial^2 T_{ins1}}{\partial y^2}\right)=0\end{aligned} \quad (12)$$

where A_{ins1} is the area of insulation; $h_{v,ins1-amb}$ is the convective coefficient between the insulation and the ambient; K_{ins1} is the thermal conductivity of the insulation; δ_{ins1} is the thickness of the insulation; $\left(\frac{\partial^2 T_{ins1}}{\partial x^2}+\frac{\partial^2 T_{ins1}}{\partial y^2}\right)$ is the temperature distribution of insulation.

3.1.3 ST

The heat transfer process of ST system is similar to PVT system, mainly divided into: (1) glass cover; (2) absorber; (3) tube; (4) circulating water; and (5) insulation. The energy balance equation of each layer is expressed as follows:

■ Glass cover: The glass cover absorbs a small part of solar energy and it also has radiative and convective heat transfer with the ambient and absorber. The energy balance equation is:

$$\begin{aligned}&\alpha_{gla2}G - h_{v,gla2-amb}\left(T_{gla2} - T_{amb}\right) - \left(h_{v,gla2-abs2} + h_{r,gla2-abs2}\right)\left(T_{gla2} - T_{abs2}\right)\\&-h_{r,gla2-sky}\left(T_{gla2} - T_{sky}\right) + K_{gla2}\delta_{gla2}\left(\frac{\partial^2 T_{gla2}}{\partial x^2} + \frac{\partial^2 T_{gla2}}{\partial y^2}\right) = 0\end{aligned} \tag{13}$$

where α_{gla2} is the absorptivity of the glass cover; $h_{v,gla2-amb}$ is the convective coefficient between the glass cover and the ambient; $h_{v,gla2-abs2}$ and $h_{r,gla2-abs2}$ are the convective and radiative coefficients between the glass cover and absorber; $h_{r,gla2-sky}$ is the radiative coefficient between the glass cover and the sky; T_{gla2}, T_{amb}, T_{abs2} and T_{sky} are the temperature of glass cover, ambient, PV panel and the sky equivalent temperature; K_{gla2} is the thermal conductivity of the glass cover; δ_{gla2} is the thickness of the glass cover; $\left(\frac{\partial^2 T_{gla2}}{\partial x^2} + \frac{\partial^2 T_{gla2}}{\partial y^2}\right)$ is the temperature distribution of the glass cover.

■ ST absorber: The absorber can also absorb part of the solar energy projected from the glass cover, and there is radiative and convective heat exchange between the absorber and the glass cover, the tube and the insulation, respectively. The energy conservation equation is:

$$\begin{aligned}&\alpha_{abs2,e}G + \left(h_{v,gla2-abs2} + h_{r,gla2-abs2}\right)\left(T_{gla2} - T_{abs2}\right) - h_{c,abs2-ins2}\left(T_{abs2} - T_{ins2}\right)\\&-\frac{A_{abs2-tub2}}{A_{abs2}}h_{c,abs2-tub2}\left(T_{abs2} - T_{tub2}\right) + K_{abs2}\delta_{abs2}\left(\frac{\partial^2 T_{abs2}}{\partial x^2} + \frac{\partial^2 T_{abs2}}{\partial y^2}\right) = 0\end{aligned} \tag{14}$$

where $\alpha_{abs2,e}$ is the effective absorptivity of the collector, and the expression is:

$$\alpha_{abs2,e} = \tau_{gla2}\alpha_{abs2} \tag{15}$$

In addition, $h_{v,gla2-abs2}$ and $h_{r,gla2-abs2}$ are the convective and radiative coefficients between the glass cover and the absorber, respectively; $h_{c,abs2-ins2}$ is the conductive coefficient between absorber and insulation; $h_{c,abs2-tub2}$ is the conductive coefficient between absorber and tube; $A_{abs2-tub2}$ is the contact area between absorber and tube; A_{abs2} is the area of absorber; K_{abs2}, δ_{abs2} and $\left(\frac{\partial^2 T_{abs2}}{\partial x^2} + \frac{\partial^2 T_{abs2}}{\partial y^2}\right)$ are the thermal conductivity, thickness and temperature distribution of the absorber respectively; T_{gla2}, T_{abs2}, T_{tub2} and T_{ins2} are the temperature of the glass cover, absorber, tube and insulation respectively.

■ Tube: There is conductive heat exchange between the tube and the absorber and insulation respectively, and there is convective heat exchange with the circulating water. The energy conservation equation of one of the water pipes is:

$$\begin{aligned}&A_{abs2-tub2}h_{c,abs2-tub2}\left(T_{abs2} - T_{tub2}\right) - A_{tub2-ins2}h_{c,tub2-ins2}\left(T_{tub2} - T_{ins2}\right)\\&-A_{tub2-flu2}h_{v,tub2-flu2}\left(T_{tub2} - T_{flu2}\right) + K_{tub2}\frac{\pi\left(D_0^2 - D_i^2\right)}{4}\frac{d^2 T_{tub2}}{dy^2} = 0\end{aligned} \tag{16}$$

where $h_{c,abs2-tub2}$ represents the conductive coefficient between absorber and tube; $h_{c,tub2-ins2}$ represents the conductive coefficient between tube and insulation; $A_{tub2-ins2}$ and $A_{tub2-flu2}$ respectively represent the contact area of tube and insulation and the contact area of tube and fluid; T_{flu2} represents the temperature of fluid; K_{tub2} represents the thermal conductivity of tube; represents the temperature distribution of tube.

■ Circulating water: There is only convective heat exchange between the circulating water and the tube, and the energy conservation equation is:

$$A_{tub2-flu2}h_{v,tub2-flu2}\left(T_{tub2} - T_{flu2}\right) - C_{flu2}\dot{m}_{flu2}\frac{dT_{flu2}}{dy} = 0 \tag{17}$$

where C_{flu2} is the heat capacity of fluid; $\dot{m}_{flu2}$ is the mass flow of fluid; $\frac{dT_{flu2}}{dy}$ is the temperature distribution of fluid.

■ Insulation: There is conductive heat exchange between the insulation and the absorber and tube, and there is convective and radiative heat exchange with the ambient. The energy conservation equation is:

$$\begin{aligned}&\frac{A_{tub2-ins2}}{A_{ins2}}h_{c,tub2-ins2}\left(T_{tub2} - T_{ins2}\right) + h_{c,abs2-ins2}\left(T_{abs2} - T_{ins2}\right)\\&-h_{v,ins2-amb}\left(T_{ins2} - T_{amb}\right) + K_{ins2}\delta_{ins2}\left(\frac{\partial^2 T_{ins2}}{\partial x^2} + \frac{\partial^2 T_{ins2}}{\partial y^2}\right) = 0\end{aligned} \tag{18}$$

where A_{ins2} is the area of insulation; $h_{v,ins2-amb}$ is the convective coefficient between the insulation and the ambient; K_{ins2} is the thermal conductivity of the insulation; δ_{ins2} is the thickness of the insulation; $\left(\frac{\partial^2 T_{ins2}}{\partial x^2} + \frac{\partial^2 T_{ins2}}{\partial y^2}\right)$ is the temperature distribution of insulation.

The area in the above formulas is the area under unit length, where. $A_{abs} = A_{ins}, A_{abs-tub} \approx D_0, T_{abs-ins} \approx \left(1 + \frac{\pi}{2}\right) D_0, A_{tub-flu} = \pi D_i$

3.2 Heat transfer coefficient

3.2.1 Conductive heat transfer coefficient

The thermal conductivity between two closely adjacent layers i and j is obtained from the reference [19] and expressed as:

$$h_{c,i-j} = \frac{1}{\frac{\delta_i}{2K_i} + \frac{\delta_j}{2K_j}} \tag{19}$$

3.2.2 Convective heat transfer coefficient

The system has three different types of convective coefficients, namely: (1) boundary surface and ambient; (2) between internal layers; (3) between water and tube [20–22].

(1) The convective heat transfer between the glass cover and the ambient is mainly related to wind speed, and the empirical formula [20] is expressed as:

$$h_{v,gla-amb} = 2.8 + 3.0V_{wind} \tag{20}$$

where V_{wind} represents the wind speed, and the default wind speed is 2 m~~m~~/s.

(2) The convective heat transfer at the air duct can be regarded as natural convection, which is related to the air duct parameters. The formula is given in Ref. [21]:

$$h_{v,gla-pv} = \frac{Nu_a \cdot K_a}{\delta_a} \tag{21}$$

The Nusselt number Nu_a here is expressed by the empirical formula as [22]:

$$Nu_a = 1 + 1.44\left(1 - \frac{1708}{Ra\delta_a \cos\beta}\right)^+ \left[1 - \frac{1708(\sin 1.8\beta)^{1.6}}{Ra\cos\beta}\right] + \left[\left(\frac{Ra\cos\beta}{5830}\right)^{1/3} - 1\right]^+ \tag{22}$$

where β is the inclination angle. The formula is valid when the inclination angle is between 0° and 75°. The inclination angle of this study is 30°, which meets the conditions. In the formula, + means that only positive values are considered. In addition, the Rayleigh number Ra can be expressed as:

$$\mathrm{Ra} = \frac{g\alpha_v \Delta t \delta_a^3}{a\mu} \tag{23}$$

In the formula, g is the acceleration of gravity; α_v is the volume expansion coefficient; Δt is the temperature difference; δ_a is the thickness of the duct; a is the thermal diffusivity; μ is the kinematic viscosity.

(3) The convective heat transfer coefficient between water and pipe is expressed as

$$h_{v,tub-flu} = \frac{Nu_f \cdot K_f}{D_i} \tag{24}$$

The Nusselt number Nu_f here is calculated according to the estimation formula of Bejan et al. [23]:

$$\begin{aligned} Nu_f &= 4.364, \mathrm{Re} \le 2300 \\ Nu_f &= 0.023\mathrm{Re}^{0.8}\mathrm{Pr}^{0.4}, \mathrm{Re} \ge 2300 \end{aligned} \tag{25}$$

where the Reynolds number Re can be expressed as

$$\mathrm{Re} = \frac{4\dot{m}_{flu}d}{\pi D_i^2 \mu} \tag{26}$$

where d is the characteristic length, here is the length of the tube; μ is the fluid kinematic viscosity.

3.2.3 Radiative heat transfer coefficient

The radiative coefficient includes: (1) between the glass cover and the sky; (2) between the glass cover and the PV module; (3) between the glass cover and absorbers in the ST module. It is represented by the following equation:

(1) The radiative heat transfer coefficient between the glass cover and the sky is expressed as [24]:

$$h_{r,gla-sky} = \varepsilon_{gla}\sigma\left(T_{gla}^2 + T_{sky}^2\right)\left(T_{gla} + T_{sky}\right) \tag{27}$$

where ε_{gla} represents the emissivity of the glass cover; σ represents the black body radiation constant, $5.67 \times 10^{-8}\mathrm{W/(m^2 \cdot K^4)}$.

(2) The radiative coefficient between the glass cover and PV is expressed as [19]:

$$h_{r,gla-pv} = \frac{\sigma\left(T_{gla}^2 + T_{pv}^2\right)\left(T_{gla} + T_{pv}\right)}{\frac{1}{\varepsilon_{gla}} + \frac{1}{\varepsilon_{pv}} - 1} \tag{28}$$

where ε_{pv} represents the emissivity of the PV module.

(3) Similarly, the radiative coefficient between the glass cover and the ST collector can be expressed as:

$$h_{r,gla-abs} = \frac{\sigma\left(T_{gla}^2 + T_{abs}^2\right)\left(T_{gla} + T_{abs}\right)}{\frac{1}{\varepsilon_{gla}} + \frac{1}{\varepsilon_{abs}} - 1} \tag{29}$$

where ε_{abs} represents the emissivity of absorber.

3.3 Performance evaluation criteria

The electrical efficiency is the ratio of photovoltaic module electricity generation to total incident solar radiation, is calculated as follows:

$$\eta_e = \frac{E_{ele,tot}}{A_c G} \tag{30}$$

where $E_{ele,tot}$ represents electrical generation, G represents solar radiation, A_c represents collector area. It should be noted that the area of PVT-ST is constant, while that of PV-ST is variable.

The thermal efficiency is the ratio of the total thermal energy absorbed by the system to the total incident solar radiation of the system, calculated as follows:

$$\eta_h = \frac{Q_h}{2A_c G} \tag{31}$$

where the total thermal energy (Q_h) collected by the system is taken away by the water in the tubes and is calculated by the following formula:

$$Q_h = \dot{m}_{flu} C_{flu}\left(T_o - T_i\right) \tag{32}$$

where $\dot{m}_{flu}$ represents mass flow rate of fluid, C_{flu} represents heat capacity of fluid, T_o represents outlet water temperature, T_i represents inlet water temperature.

Primary energy saving efficiency, accounting for the overall performance of both the quantity and quality of energy output for a system, is described as [25]:

$$\eta_f = \frac{\eta_e}{\eta_{power}} + \eta_h \tag{33}$$

where η_{power} is the conversion efficiency of electrical generation for conventional power plants, which is primarily considered as 38 % [26] in the current research.

In addition, two statistical indicators, root mean square deviation (RMSD) and relative error (RE), are used to verify the numerical model through reference results. The calculation method of RE is:

$$RE = \left| \frac{R_{ref,i} - R_{sim,i}}{R_{ref,i}} \right| \times 100\% \tag{34}$$

and RMSD is taken by:

$$RMSD = \sqrt{\frac{\sum \left[100 \times \left(R_{ref,i} - R_{sim,i}\right) / \left(R_{ref,i}\right)\right]^2}{N_{\exp}}} = \sqrt{\frac{\sum \left[100 \times RE\right]^2}{N_{\exp}}} \tag{35}$$

where $R_{ref,i}$ represents the reference results at the point of i, $R_{sim,i}$ represents simulation results at the point of i, $N_{\exp}$ represents the number of reference points conducted.

3.4 Numerical simulation procedure

Gambit is used to mesh the physical model. All the calculation areas are structured grids, and the boundary layer grids are added near the tube for encryption. The mesh number of PVT component model is 476,740, ST component model is 304,600 and PV component model is 146,400.927,740 of grid number is adopted to simulate after an independent mesh evaluation. Due to the small hydraulic diameter of the cooling channel, the flow state of the cooling fluid is laminar. Therefore, the turbulence model uses the default laminar flow model to calculate the flow process. Furthermore, the radiation model adopts the DO model. The mass inflow inlet and pressure outlet boundary conditions are adopted as the import and export boundary conditions. The solar radiation input is equivalent to a user-defined heat flux function. User defined function based on thermal balance equation of photovoltaic module is connected to the Fluent solver through an “interpret” method, and the bottom and other walls before and after using adiabatic boundary conditions. The Pressure-velocity coupling scheme is set as SIMPLEC. The Second Order Upwind scheme applies to momentum and energy.

With the help of Fluent software, the control volume method and a transient model was used to solve the problem. When the residual is lower than a certain standard (the residual standard of the energy equation is 10^{-6}, and the remaining equations is 10^{-3}), and the monitoring point is relatively stable or the fluctuation is small, the calculation result is considered to be convergent, and the simulated steady state solution is obtained. The procedure of numerical simulation developed in this research is illustrated in Fig. 6.

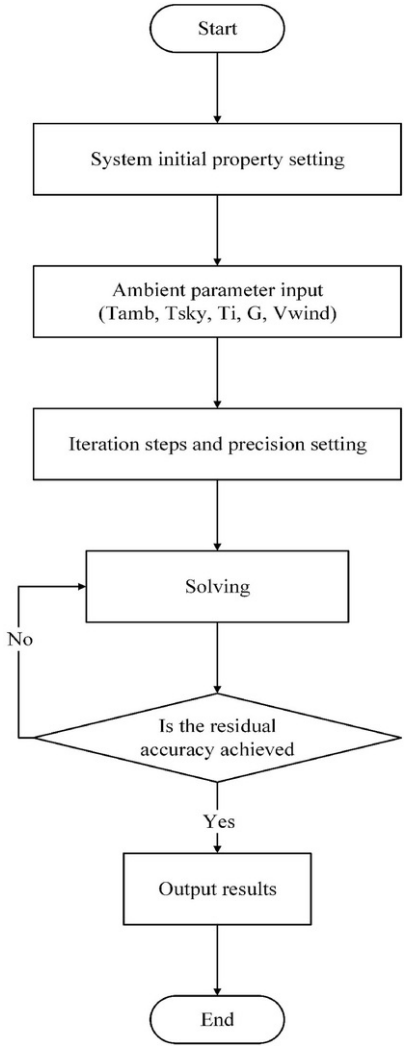

Fig. 6 Procedure of numerical simulation for the system.

alt-text: Fig. 6

In addition, the validity of the model is verified in this study, and the structural parameters and working conditions are the same as the data in the references. The simulation of PV/T in paper [18] is set as solar radiation level of 1000 W/m^2, wind speed of 2 m/s, water flow rate of 0.04 kg/s, both the inlet water and ambient temperature of 298.15 K.

According to the simulated data under different environmental conditions, Figs. 7–11 is drawn using Origin 2017.

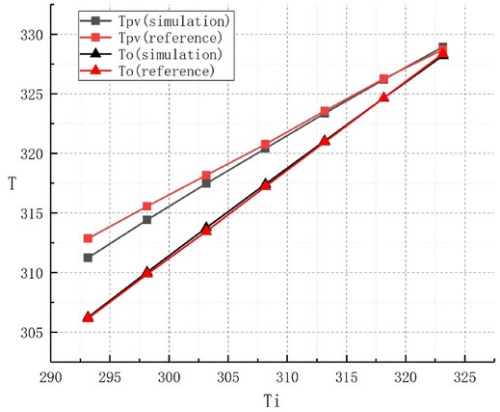

Fig. 7 Comparison of PV temperature and outlet water temperature between simulation results and references at different inlet water temperature.

alt-text: Fig. 7

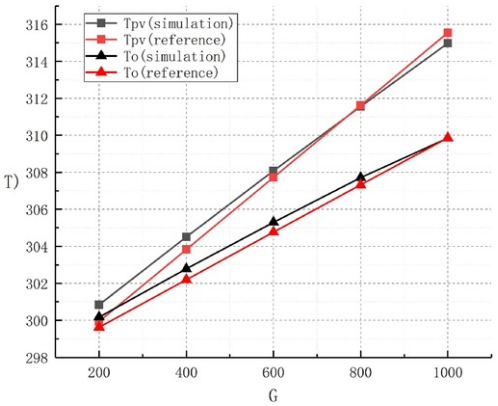

Fig. 8 Comparison of PV temperature and outlet water temperature between simulation results and references under different solar radiation.

alt-text: Fig. 8

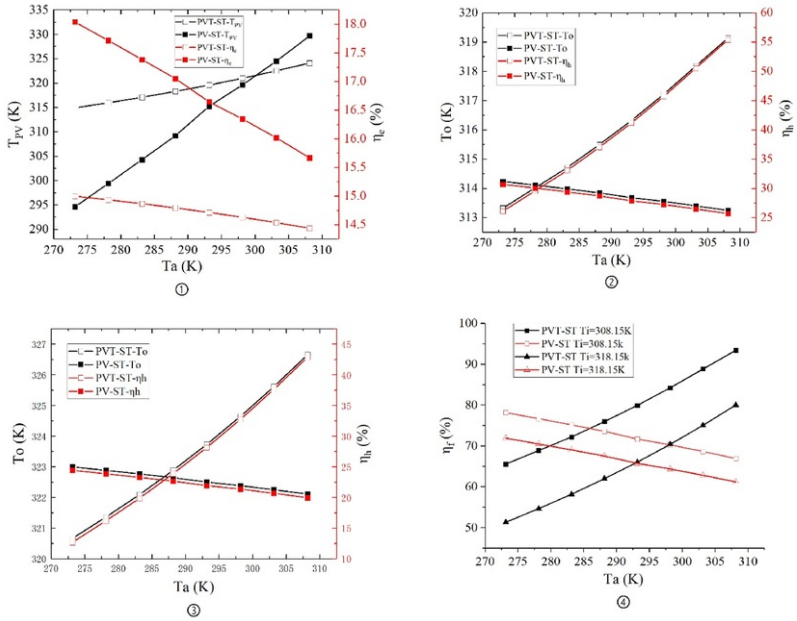

Fig. 9 Comparison of performance of PVT-ST and PV-ST systems at different ambient temperatures.

alt-text: Fig. 9

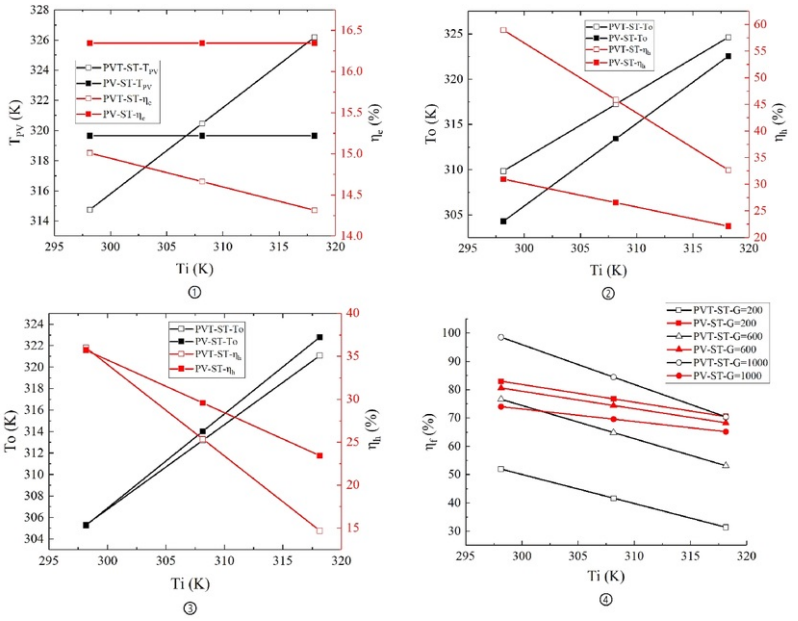

Fig. 10 Comparison of performance of PVT-ST and PV-ST systems at different inlet temperatures.

alt-text: Fig. 10

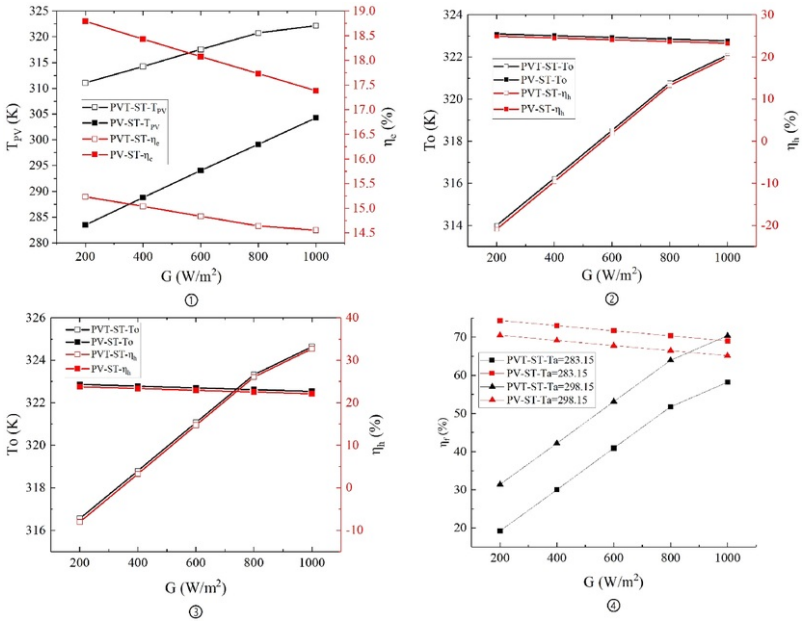

Fig. 11 Comparison of performance of PVT-ST and PV-ST systems under different solar radiation.

alt-text: Fig. 11

4 Model validation

In this study, the area of the PVT module and the ST module are fixed for the PVT-ST system. Because the same amount of electricity is generated, the PV area of the PV-ST system is changed and only the total area is maintained constant. The thermo-physical parameters of different layers of the two systems are listed in Table 2.

Table 2 Thermo-physical properties of different layers of the PVT-ST and PV-ST system [24,27].

alt-text: Table 2

Components	Parameters	Values	Units
Glass cover	Density, ρ	2200	kg/m^3
	Thermal conductivity, K	0.9	W/(m•k)
	Specific heat capacity, C	670	J/(kg•k)
	Absorptivity, α_{gla}	0.02	–
	Transmittance, τ_{gla}	0.9	–
	Emissivity, ε_{gla}	0.9	–
Air gap	Density, ρ	1.185	kg/m^3
	Thermal conductivity, K	0.0263	W/(m•k)

	Specific heat capacity, C	1005	J/(kg•k)
	Thickness, δ_a	0.025	m
PV	Density, ρ	2330	kg/m³
	Thermal conductivity, K	140	W/(m•k)
	Specific heat capacity, C	900	J/(kg•k)
	Emissivity, ε_{pv}	0.88	–
	Absorptivity, α_{pv}	0.81	–
	Transmittance, τ_{pv}	0.06	–
Absorber	Density, ρ	2702	kg/m³
	Thermal conductivity, K	310	W/(m•k)
	Specific heat capacity, C	880	J/(kg•k)
	Absorptivity, α_{abs}	0.95	–
	Emissivity, ε_{abs}	0.88	–
Tube	Density, ρ	8920	kg/m³
	Thermal conductivity, K	377	W/(m•k)
	Specific heat capacity, C	386	J/(kg•k)
	Diameter, D	0.01	m
Heat transfer fluid	Density, ρ	996.95	kg/m³
	Thermal conductivity, K	0.61	W/(m•k)
	Specific heat capacity, C	4178.5	J/(kg•k)
Insulation	Density, ρ	230	kg/m³
	Thermal conductivity, K	0.025	W/(m•k)
	Specific heat capacity, C	1670	J/(kg•k)

In addition, the entire PV module is considered as a whole component in order to simplify the calculation and its nominal efficiency is 17.8 %. The temperature coefficient of photovoltaic modules is −0.38 %. The parameters indicated by the PV module in Table 1 are the parameters of the overall component.

Ma et al. [18] proposed an innovative integrated system called PVT-ST that connected PVT modules in series with subsequent solar thermal (ST) absorbers, which was modeled based on experimental data. The results show that the numerical results are in good agreement with the collected data, and the root mean square deviation is less than 1.39 %. This article uses this as a reference to compare the data results. Figs. 7 and 8 show the comparison between the simulation results and the reference results under different inlet water temperature and solar radiation respectively.

It can be seen from Fig. 7 that under different inlet water temperature conditions, the relative error of PV temperature is between 0.02 % and 0.52 %; the relative error of outlet water temperature is between 0.0039 % and

0.094 %. The root mean square deviation of PV temperature is 0.258 %; the root mean square deviation of outlet water temperature is 0.054 %.

It can be seen from Fig. 8 that under different solar radiation conditions, the relative error of PV temperature is between 0.02 % and 0.3 %; the relative error of outlet water temperature is between 0.002 % and 0.194 %; the root mean square deviation of PV temperature is 0.193 %; the root mean square deviation of outlet water temperature is 0.153 %.

When the solar radiation is low, the maximum relative errors of photovoltaic temperature and outlet water temperature are 0.3 % and 0.194 %. As the inlet water temperature increases, the relative errors of PV temperature and outlet water temperature are shrinking. Therefore, the model is more accurate at higher inlet water temperature.

In summary, under different inlet water temperature and different solar irradiance conditions, the simulation results of PV temperature (Tpv) and outlet water temperature (To) are in good agreement with the reference results. The verification shows that the model has excellent performance and can be used for future simulation work.

5 Results and discussion

The performance of PVT-ST and PV-ST depends on many factors. This section will discuss in detail the influence of several parameters such as ambient temperature, inlet water temperature and solar radiation on the two systems. It should be emphasized that the following results are all based on the conditions of the same total receiving area of the two systems for comparison.

5.1 Different ambient temperature

Fig. 9 shows the performance comparison of PVT-ST and PV-ST systems at different ambient temperatures. Fig. 1 and 2 show the performance comparison of PVT-ST and PV-ST systems at different ambient temperatures when the solar radiation G = 1000 W/m^2 and the inlet temperature Ti = 308.15 K.Fig. 3 shows the comparison of outlet water temperature and thermal efficiency of PVT-ST and PV-ST systems at different ambient temperatures when solar radiation G = 1000 W/m^2 and inlet temperature Ti = 318.15 K. Fig. 4 shows the comparison of primary energy saving efficiency of PVT-ST and PV-ST systems under different ambient temperatures when solar radiation G = 1000 W/m^2 and inlet temperature Ti = 308.15 K and Ti = 318.15 K, respectively.

It can be seen from Fig. 1 that, with the increase of ambient temperature, the PV temperature of both systems will increase, which is obvious. This is because the higher the ambient temperature, the less heat is lost by the system through the environment, and the more heat is carried away by the water, thus the higher the outlet temperature. It is worth noting that the PV temperature of the PV-ST system is lower than the PV temperature of the PVT-ST system when the ambient temperature is below 300 K. It is well known that the lower the PV temperature, the higher the electrical efficiency. Therefore, when the ambient temperature is low, the electrical efficiency of PV-ST system is greater than that of PVT-ST system. Moreover, the lower the ambient temperature, the lower the PV temperature of the relative PV-ST system. This is because the PV components of the PV-ST system directly exchange heat with the environment and are greatly affected by the ambient temperature. The lower the ambient temperature, the more obvious the decrease in the PV temperature will be. This indicates that the electrical efficiency per unit area of the PV-ST system is higher than that of the PVT-ST system at lower ambient temperatures. At this point, the PV-ST system has more advantages in electrical efficiency.

Figs. 2 and 3 respectively show the comparison of outlet water temperature and thermal efficiency of the two systems under different ambient temperatures when the inlet temperature is 308.15 K and 318.15 K. It can be seen that the outlet water temperature of the PVT-ST system will increase with the increase of the ambient temperature. This is because the higher the ambient temperature, the less heat the system will lose through the ambient, and more heat will be taken away by water, therefore the outlet water temperature will be higher. The outlet water temperature for the PV-ST system does not rise but decreases as the ambient temperature increases. This is because the PV module of the PV-ST system directly exchanges heat with the ambient, which is greatly affected by the ambient temperature. Low ambient temperature will make the area of PV required to generate the same electricity as the PVT-ST system smaller, and the area of ST module used to heat water will be larger, so the outlet water temperature will rise slightly.

At lower temperatures, the water outlet temperature and thermal efficiency of the PV-ST system are both higher. When the temperature is higher, the effluent temperature and thermal efficiency of the PVT-ST system are higher. Moreover, it can be seen from ②③ comparison that the higher the inlet temperature is, the more obvious the advantage of outlet water temperature of the PV-ST system is under low temperature.

Fig. 4 shows the comparison of the primary energy saving efficiency of the two systems under different environmental temperature conditions when the inlet temperature is 308.15 K and 318.15 K. It can be seen that the PV-ST system have more advantages in low temperature environment, and the higher the inlet temperature is, the more obvious this low temperature advantage of the PV-ST system is. In real life, the temperature of circulating water should be increasing and will stabilize at a higher temperature, when the PV-ST system will be more advantageous.

In general, the lower the ambient temperature, the more advantages the PV-ST system has, and the higher the ambient temperature, the more advantages the PVT-ST system has.

5.2 Different inlet water temperature

Fig. 10 shows the performance comparison of PVT-ST and PV-ST systems at different inlet temperatures. Fig. 1 and 2 show the performance comparison of PVT-ST and PV-ST systems at different inlet temperatures when the ambient temperature is Ta = 298.15 K and the solar radiation intensity is G = 1000 W/m^2. Fig. 3 shows the comparison of outlet temperature and thermal efficiency of the two systems at different inlet temperatures when the ambient temperature is Ta = 298.15 K and the solar radiation intensity is G = 600 W/m2. Fig. 4 shows the comparison of primary energy saving efficiency of the two systems at different inlet temperatures when the ambient temperature is Ta = 298.15 K and the solar radiation intensity is G = 200 W/m^2, G = 600 W/m^2 and G = 1000 W/m^2, respectively.

Because the cooling water of the whole system is constantly circulating, and the water temperature will keep rising in this process, it is particularly important to study the performance of the system under different inlet temperatures.

Fig. 10 shows the performance comparison of the two systems at different inlet temperatures. As can be seen from Fig. 1, the increase of inlet water temperature leads to the deterioration of PV heat transfer of the PVT-ST system, thus leading to the rise of temperature. The PV components of the PV-ST system rely on the air to exchange heat and are not affected by the circulating water, so the PV temperature remains constant.

Based on Fig. 2, at G = 1000 W/m^2, the effluent temperature also increases with the increase of inlet temperature, but the thermal efficiency decreases. Moreover, the effluent temperature and thermal efficiency of the PVT-ST system are higher than that of the PV-ST system when the solar radiation is strong. It is worth noting that, based on the results shown in Fig. 3, at G = 600 W/m^2, it can be seen that the effluent temperature and thermal efficiency of the PVT-ST system are lower than those of the PV-ST system when the solar radiation is low. This indicates that the performance of the PV-ST system is better than that of the PVT-ST system at lower solar radiation.

Fig. 4 shows that the primary energy saving efficiency of the PV-ST system is better than that of the PV-ST system at G = 1000 W/m^2. When G = 600 W/m^2, the primary energy saving efficiency of PVT-ST system is lower than that of PV-ST system.

In conclusion, as can be seen from the above four figures, the influent temperature changes have little influence on the PV-ST system, but great influence on the PVT-ST system.

5.3 Different solar radiation

Fig. 11 shows the comparison of performance of PVT-ST and PV-ST systems under different solar radiation. Fig. 1 and ② show the performance comparison of the two systems under different solar radiation when the ambient temperature Ta = 298.15 K and the inlet temperature Ti = 318.15 K. Fig. 3 shows the performance comparison of the two systems under different solar radiation when the ambient temperature Ta = 283.15 K and the inlet temperature Ti = 318.15 K. Fig. 4 shows the comparison of primary energy saving efficiency of the two systems under different solar radiation when the ambient temperature is Ta = 283.15 K and Ta = 298.15 K, respectively, and the inlet temperature Ti = 318.15 K.

Based on the results shown in ~~Fig. 1~~Fig. 1, with the increase of solar radiation intensity, PV temperature also gradually increases, leading to the decrease of battery efficiency, this is because the increase of solar radiation intensity makes the solar radiation absorbed by PV convert more energy into heat. In addition, it is worth noting that the PV temperature of the PV-ST system is significantly lower than that of the PVT-ST system when the ambient temperature is 298.15 K, because the PV components of the PV-ST system directly exchange heat with the environment, and the lower the ambient temperature, the more obvious this low temperature advantage will be.

It can be seen from Fig. 2 that the outlet water temperature of the PVT-ST system increases with the increase of solar radiation. This is because the solar energy absorbed by solar panels and ST absorbers will increase with the increase of solar radiation, so the outlet water temperature will also be higher. However, the outlet water temperature of the PV-ST system does not increase with the increase in solar radiation. This is because the increase of solar radiation leads to the rise of photovoltaic cell temperature and the decrease of electrical efficiency. The PV area required for the PV module to generate the same amount of electricity as the PVT-ST system has increased slightly. This leads to a reduction in the ST area, which in turn causes the outlet water temperature to drop instead of rising.

The PV module area required by the PV-ST system at low temperatures will be smaller than the PV module area required by the PVT-ST system on the premise that the power generation and total area remain the same. Thus, the ST area of the PV-ST system will be larger, and the effluent temperature and thermal efficiency will be better, which are also reflected in Fig. 2. When the ambient temperature is high, such as Ta = 298.15 K, this advantage is not obvious. As you can see, The outlet water temperature and thermal efficiency of the PV-ST system will be higher than that of the PVT-ST system only when G is greater than 800 W/m^2. And When G is lower than 800 W/m^2, the effluent temperature and thermal efficiency of PVT-ST system are better. However, when the ambient temperature is low, such as Ta = 283.15 K, this advantage will be obvious. As you can see, It can be seen that when G is lower than 1000 W/m^2, the effluent temperature and thermal efficiency of the PV-ST system have absolute advantages.

Fig. 4 shows the comparison of the primary energy saving efficiency of the two systems when the ambient temperature is 283.15 K. Due to the good heat dissipation performance of the PV-ST system, the primary energy saving efficiency of the PV-ST system is higher than that of the PVT-ST system, and the lower the solar radiation intensity, the more obvious this phenomenon is.

In conclusion, when the solar radiation intensity is low, the PV-ST system has more advantages, while when the solar radiation intensity is high, the PVT-ST system has more advantages.

6 Conclusion

This paper introduces the PVT-ST system, which operates in PV and ST separately, and compares the PVT-ST system which operates in series with PVT and ST. The original PVT-ST system has certain deficiencies under the conditions of low ambient temperature and high inlet water temperature. In this study, PVT was replaced by common PV without a cover. The common PV cooling effect without a cover will be better in the conditions of low ambient temperature. The area of the PV module with higher electrical efficiency will be smaller. While keeping the total area of the two systems equal, their respective application ranges are discussed.

Both systems are modelled using Gambit and simulated using Fluent. The new model was verified with the simulation results of the original PVT-ST system as a reference. The influences of ambiental temperature, inlet water temperature and solar radiation on the thermal and electrical performance of the system are analyzed in detail. The results are as follows:

(1) While keeping the total area and electricity generation equal, the lower the ambient temperature (Ta) and the higher the inlet water temperature (Ti), the outlet water temperature of the PV-ST system is higher than that of the PVT-ST system. That is, the PV-ST system has more advantages. Especially when the ambient temperature is lower than 15 °C and the inlet water temperature is greater than 45 °C, the advantages of the PV-ST system are more obvious. When the ambient temperature is greater than 30 °C and the inlet water temperature is less than 40 °C, the PVT-ST system has more advantages.

(2) The PVT-ST system can provide hot water at a higher temperature than the PV-ST system by increasing solar radiation. That is, under high radiation, the PVT-ST system has more advantages, but this advantage will gradually decrease as the inlet water temperature increases.

(3) The higher the ambient temperature and the inlet water temperature, the worse the cooling effect of PV and the less electric is generated. The greater the intensity of solar radiation, the more solar energy is absorbed, and the more power is generated.

This study also has certain shortcomings, such as the lack of annual performance evaluation of the system and the evaluation of economic indicators. In future research, we will consider adding the annual performance evaluation to discuss the influence of seasonal factors on the system.

Declaration of competing interest

The authors declare that they have no known competing financial interests or personal relationships that could have appeared to influence the work reported in this paper.

Acknowledgements

The authors would like to acknowledge our appreciation for the financial support received from the following projects: ‘A low carbon heating system for existing public buildings employing a highly innovative multiple-throughout-flowing micro-channel solar-panel-array and a novel mixed indoor/outdoor air source heat pump’ funded by the UK BEIS.

References

[1] N. Khordehgah, A. Żabnieńska-Góra and H. Jouhara, Energy performance analysis of a PV/T system coupled with domestic hot water system, *Chem Eng* **4**, 2020, 22.

[2] G. Li, Q. Xuan, G. Pei, Y. Su and J. Ji, Effect of non-uniform illumination and temperature distribution on concentrating solar cell - a review, *Energy* **144**, 2018, 1119–1136.

[3] Q. Xuan, G. Li, Y. Lu, B. Zhao, X. Zhao and G. Pei, The design, construction and experimental characterization of a novel concentrating photovoltaic/daylighting window for green building roof, *Energy* **175**, 2019, 1138–1152.

[4] C. Peng, Y. Huang and Z. Wu, Building-integrated photovoltaics (BIPV) in architectural design in China, *Energy Build* **43**, 2011, 3592–3598.

[5] M.S. Guney, Solar power and application methods, *Renew Sustain Energy Rev* **57**, 2016, 776–785.

[6] J. Urbanetz, C.D. Zomer and R. Rüther, Compromises between form and function in grid-connected, building-integrated photovoltaics (BIPV) at low-latitude sites, *Build Ambient* **46**, 2011, 2107–2113.

[7] H.A. Zondag, D.W. Vries and A.A. Van Steenhoven, Thermal and electrical yield of a combipanel. ISES solar world Congress, *Jerus Isr* 1999, 4–9.

[8] W. Pang, Y. Zhang, B.C. Duck, H. Yu, X. Song and H. Yan, Cross sectional geometries effect on the energy efficiency of a photovoltaic thermal module: numerical simulation and experimental validation, *Energy* **209**, 2020, 118439.

[9] M. Dhimish, Thermal impact on the performance ratio of photovoltaic systems: a case study of 8000 photovoltaic installations, *Case Studies Thermal Eng.* **21**, 2020, 100693.

[10] C. El Fouas, B. Hajji, A. Gagliano, G.M. Tina and S. Aneli, Numerical model and experimental validation of the electrical and thermal performances of photovoltaic/thermal plant, *Energy Convers Manag* **220**, 2020, 112939.

[11] G. Barone, A. Buonomano, C. Forzano, G.F. Giuzio and A. Palombo, Passive and active performance assessment of building integrated hybrid solar photovoltaic/thermal collector prototypes: energy, comfort, and economic analyses, *Energy* **209**, 2020, 118435.

[12] V. Sun, A. Asanakham, T. Deethayat and T. Kiatsiriroat, A new method for evaluating nominal operating cell temperature (NOCT) of unglazed photovoltaic thermal module, *Energy Rep* **6**, 2020, 1029–1042.

[13] D. Das, P. Kalita, A. Dewan and S. Tanweer, Development of a novel thermal model for a PV/T collector and its experimental analysis, *Sol Energy* **188**, 2019, 631–643.

[14] K. Kant, A. Shukla, A. Sharma and P.H. Biwole, Thermal response of poly-crystalline silicon photovoltaic panels: numerical simulation and experimental study, *Sol Energy* **134**, 2016, 147–155.

[15] M.M. Sardouei, H. Mortezapour and K. Jafari Naeimi, Temperature distribution and efficiency assessment of different PVT water collector designs, *Sādhanā* **43**, 2018, 84.

[16] P. Singh and N.M. Ravindra, Temperature dependence of solar cell performance—an analysis, *Sol Energy Mater Sol Cell* **101**, 2012, 36–45.

[17] E. Skoplaki and J.A. Palyvos, On the temperature dependence of photovoltaic module electrical performance: a review of efficiency/power correlations, *Sol Energy* **83**, 2009, 614–624.

[18] T. Ma, M. Li and A. Kazemian, Photovoltaic thermal module and solar thermal collector connected in series to produce electricity and high-grade heat simultaneously, *Appl Energy* **261**, 2020, 114380.

[19] W.C. Swinbank, Long-wave radiation from clear skies, *Q J R Meteorol Soc* **89**, 2010, 339–348.

[20] J.A. Duffie, W.A. Beckman and J. Mcgowan, Solar engineering of thermal processes, *WileyIntersci Publ* **116**, 2006, 549.

[21] J.H. Watmuff, W.W.S. Charters and D. Proctor, Solar and wind induced external coefficients – solar collectors, *Cooperation Mediterraneenne Pour Lenergie Solaire* **1**, 1977, 56.

[22] K.G.T. Hollands, T.E. Unny, G.D. Raithby and L. Konicek, Free convective heat transfer across inclined air layers, *J Heat Tran* **98**, 1976, 189–193.

[23] A. Bejan, Convection heat transfer, 2013, John wiley & sons.

[24] O. Rejeb, H. Dhaou and A. Jemni, A numerical investigation of a photovoltaic thermal (PV/T) collector, *Renew Energy* **77**, 2015, 43–50.

[25] B.J. Huang, T.H. Lin, W.C. Hung and F.S. Sun, Performance evaluation of solar photovoltaic/thermal systems, *Sol Energy* **70**, 2001, 443–448.

[26] M. Ghadiri, M. Sardarabadi, M. Pasandideh-Fard and A.J. Moghadam, Experimental investigation of a PVT system performance using nano ferrofluids, *Energy Convers* **103**, 2015, 468–476.

[27] J.F. Chen, L. Zhang and Y.J. Dai, Performance analysis and multi-objective optimization of a hybrid photovoltaic/thermal collector for domestic hot water application, *Energy* **143**, 2018, 500–516.

Nomenclature

A_c : collector area (m^2)

C : heat capacity

K : conductivity (W/m·K)

G : solar radiation (W/m^2)

E : electricity (W)

T : temperature (K)

V_{wind} : wind local speed (m/s)

Q_h : total thermal energy

D : diameter

d : characteristic length

g : gravity

h_c : conductive coefficient (W/ m^2·K)

h_v : convective coefficient (W/m^2·K)

h_r : radiative coefficient (W/ m^2·K)

Nu : Nusselt number

Pr : Prandtl number

Ra : Rayleigh number

Re : Reynolds number

$R_{ref,i}$: reference results at the point of i

$R_{sim,i}$: simulation results at the point of i

N_{exp} : the number of experimental points conducted

Greek number

a : thermal diffusivity

α : absorptivity

α_v : coefficient of volume expansion

μ : kinematic viscosity

τ : transmittance

δ : thickness (m)

ε : emissivity

σ : Stefan-Boltzmann constant

η : efficiency (%)

γ : temperature coefficient

$\dot{m}$: mass flow rate (kg/s)

Δt: temperature difference

Subscript

c: conduction

v: convection

r: radiation

amb: ambient

sky: sky

gla: glass cover

pv: photovoltaic

abs: absorber

tub: tube

flu: fluid

ins: insulation

ele: electricity

ref: reference temperature

Abbreviation

CFD: computational fluid dynamics

PVT: photovoltaic thermal

PV: photovoltaic

ST: solar thermal

PVT-ST: photovoltaic thermal and solar thermal collector connected in series

PV-ST: photovoltaic and solar thermal collector connected in series

$RMSD$: root mean square deviation

RE : relative error

Highlights

- A new combination scheme of photovoltaic module and solar collector (PV-ST) is proposed.
- Model validation shows good agreement with reference results.
- The advantages and disadvantages of PVT-ST and PV-ST systems under different environmental conditions were compared.

Queries and Answers

Query: Please confirm that the provided email “Guiqiang.Li@hull.ac.uk” is the correct address for official communication, else provide an alternate e-mail address to replace the existing one, because private e-mail addresses should not be used in articles as the address for communication.
Answer: Yes.

Query: Have we correctly interpreted the following funding source(s) and country names you cited in your article: BEIS, United Kingdom?
Answer: Yes

Query: Please confirm that given names and surnames have been identified correctly and are presented in the desired order and please carefully verify the spelling of all authors’ names.
Answer: Yes

Query: Your article is registered as belonging to the Special Issue/Collection entitled “ Energy Advances - GCEEC”. If this is NOT correct and your article is a regular item or belongs to a different Special Issue please contact s.venkiteswaran@elsevier.com immediately prior to returning your corrections.
Answer: Yes